J. Microbiol. Biotechnol. (2017), 27(12), 2228–2236
https://doi.org/10.4014/jmb.1710.10001

jmb

Difference in the Gut Microbiome between Ovariectomy-Induced Obesity and Diet-Induced Obesity

Sungmi Choi[1†], Yu-Jin Hwang[2†], Min-Jeong Shin[1,3], and Hana Yi[1,3*]

[1]*Department of Public Health Sciences, Graduate School, Korea University, Seoul 02841, Republic of Korea*
[2]*Department of Agrofood Resources, National Institute of Agricultural Science, RDA, Wanju 54875, Republic of Korea*
[3]*School of Biosystem and Biomedical Science, Korea University, Seoul 02841, Republic of Korea*

Received: October 10, 2017
Revised: November 1, 2017
Accepted: November 7, 2017

First published online
November 9, 2017

**Corresponding author*
Phone: +82-2-3290-5644;
Fax: +;
E-mail: hanayi@korea.ac.kr

†These authors contributed equally to this work.

Supplementary data for this paper are available on-line only at http://jmb.or.kr.

pISSN 1017-7825, eISSN 1738-8872

During menopausal transition, the imbalance of estrogen causes body weight gain. Although gut microbiome dysbiosis has been reported in postmenopausal obesity, it is not clear whether there is any difference in the microbiome profile between dietary-induced obesity and postmenopausal obesity. Therefore, in this study, we analyzed intestinal samples from ovariectomized mice and compared them with those of mice with high-fat diet-induced obesity. To further evaluate the presence of menopause-specific bacteria-gene interactions, we also analyzed the liver transcriptome. Investigation of the 16S rRNA V3-V4 region amplicon sequence profile revealed that menopausal obesity and dietary obesity resulted in similar gut microbiome structures. However, *Bifidobacterium animalis* was exclusively observed in the ovariectomized mice, which indicated that menopausal obesity resulted in a different intestinal microbiome than dietary obesity. Additionally, several bacterial taxa (*Dorea* species, *Akkermansia muciniphila*, and *Desulfovibrio* species) were found when the ovariectomized mice were treated with a high-fat diet. A significant correlation between the above-mentioned menopause-specific bacteria and the genes for female hormone metabolism was also observed, suggesting the possibility of bacteria-gene interactions in menopausal obesity. Our findings revealed the characteristics of the intestinal microbiome in menopausal obesity in the mouse model, which is very similar to the dietary obesity microbiome but having its own diagnostic bacteria.

Keywords: Microbiome, menopause, obesity, ovariectomy

Introduction

During menopause, women suffer from abnormal health conditions due to a lack of female hormones. Women in menopausal transition show various symptoms that although not severe, affect daily life, including hot flashes, cold sweats, and insomnia [1]. The lack of female hormones also causes bone loss and is the leading cause of osteoporosis [2–4]. The risk of Alzheimer's disease is also known to increase during menopausal transition [5, 6].

Obesity is another problem that women face during menopausal transition. During menopause, the lack of estrogen results in an increase in body weight. Animal experiments using ovariectomized rats have shown that the increase in body weight is due to estrogen deprivation [7]. This phenomenon has also been confirmed in humans. Decreased estradiol levels have been found to induce an increase in the level of follicle-stimulating hormone, resulting in increased abdominal subcutaneous fat [8]. There are many hypotheses about the causes of menopausal obesity. The most widely known mechanism is that estrogen affects the expression of the leptin gene. Upon ovariectomy, the expression of the *ob* gene, which encodes leptin, decreases and the concentration of leptin decreases in the blood [7, 9]. Increase in visceral fat during transition to menopause also causes the metabolic syndrome [10]. Cardiovascular diseases,

high blood pressure, type 2 diabetes mellitus, and various cancers have also been reported to be caused by menopausal obesity [11–15].

Hormone replacement therapy (HRT) is widely used to prevent various chronic diseases caused by menopause and to relieve postmenopausal symptoms in a short period. Estrogen or progesterone, and recently, androgen and progestin, depending on the situation, are used for HRT [16]. HRT alleviates the symptoms of menopause in a short time and is effective in preventing osteoporotic fractures and dementia. However, HRT has side effects that cause cardiovascular diseases such as stroke and thromboembolism, and long-term HRT increases the risk of cholecystitis and breast cancer [16]. Therefore, there is an urgent need for alternative therapies; one of the alternative theories that has been proposed involves the use of intestinal bacteria, for example in the form of probiotics.

Existing microbiome studies in postmenopausal women have been focused on vaginal bacteria. During menopause, the vaginal environment changes greatly in terms of humidity and pH, which in turn changes the composition of the vaginal microbiota [17–19]. Similar changes in the microbiome depending on the postmenopausal status have also been reported in the urine and feces [20, 21]. This microbiome dysbiosis in postmenopausal women also conversely affects the regulation of systemic estrogen hormones. Multifaceted studies on the gut microbiome and estrogen levels during menopause have revealed that the estrobolome, the estrogen metabolism-related genes possessed by the microbiome, plays an important role in estrogen circulation [22, 23]. The order Clostridiales and the genus *Bacteroides* have also been reported to be correlated with the urinary estrogens level in postmenopausal women [20]. Moreover, over a hundred intestinal bacteria in postmenopausal women with obesity have been found to be correlated with metabolic risk markers, including insulin resistance, inflammation, and lipid metabolism [24].

Although there have been many studies on the microbiome profile of animal models and humans, it is not known whether postmenopausal weight gain induces the same changes in the gut microbiome as dietary-induced obesity does. Therefore, the objective of this study was to investigate the effect of menopausal body weight gain on the gut microbiome in an ovariectomized animal model in controlled experiments. To this end, we analyzed the gut microbiome of ovariectomized mice and compared it with that of mice with high-fat diet-induced obesity. In addition, we analyzed the transcriptome from liver samples to identify genes correlated with intestinal bacteria that specifically changed during menopause.

Materials and Methods

Animals and Experimental Design

Sham-operated or ovariectomized female mice (ICR) were purchased from Orient (Korea). Ovariectomy involved the surgical removal of the fallopian tubes and ovaries through a midline incision. Sham operation was a fake surgical intervention through the midline incision through the skin and muscle. The sham operation or ovariectomy was performed 2 weeks prior to arrival (at 8 weeks of age). The mice (10 weeks old) were caged individually to minimize cage-dependent bias on the microbiome. The mice were kept under controlled environmental conditions (22 ± 2°C, 50–60% humidity, 12-h light/dark cycle) in the Animal Care Facility at the National Institute of Agricultural Sciences (Korea). After 1 week of acclimatization, the mice were divided into four groups: SHAM (sham-operated mice; $n = 3$), OVX (ovariectomized mice; $n = 5$), SHAM-HF (sham-operated mice given a high-fat diet; $n = 3$), and OVX-HF (ovariectomized mice given a high-fat diet; $n = 5$). The low-fat diet groups (SHAM and OVX) were fed with Normal Chow diet (+40 RMM) purchased from Central Laboratory Animal, Inc. (Korea). The high-fat diet groups (SHAM-HF, OVX-HF) were fed with rodent diet with 60% Kcal fat (Research Diet, D12492). The feeding was maintained for 12 consecutive weeks. At the end of the experiments, the mice were fasted 12 h prior to sacrifice. The mice were anesthetized with CO_2 and sacrificed by exsanguination. The blood, large intestine (cecum and colon), and liver were sampled and immediately frozen in liquid nitrogen and stored at −86°C until further analysis. The study protocols were approved by the IACUC of National Institute of Agricultural Sciences (Approval No. NAAS-1506).

Biochemical Assays for Obesity-Related Indices

Total triglyceride (Abcam, UK), total cholesterol (Abcam), and high-density lipoprotein (HDL)-cholesterol (Abcam) in the blood were measured using an ELISA kit (Abcam) according to the manufacturer's instructions. Low-density lipoprotein (LDL)-cholesterol, atherogenic index (AI), and cardiac risk factor (CRF) were calculated according to Fridewald's method using the following equations:

LDL-cholesterol = total cholesterol - (HDL-cholesterol + triglyceride/5)

AI = (total cholesterol - HDL-cholesterol)/HDL-cholesterol

CRF = total cholesterol/HDL-cholesterol

Gut Microbiome Analyses

The contents of the large intestine were homogenized in sterile PBS solution using a micropestle. The homogenized sample was then filtered using a syringe filter (5 μm; MilliPore, USA) to

remove the host cells. For metagenomic DNA extraction, 200 µl of the filtrate was applied to the FastDNA Spin Kit for Soil (MP Biomedicals, USA). The 16S rRNA hypervariable regions V3-V4 were amplified following the 16S Metagenomic Sequencing Library Preparation guide provided by Illumina (USA). The gene-specific forward primer (5′-TCGTCGGCAGCGTCAGATGTGTATAAGAGACAG-CCTACGGGNGGCWGCAG; with the underline indicating the Illumina overhang adapter sequence) and reverse primer (5′-GTCTCGTGGGCTCGGAGATGTGTATAAGAGACAG-GACTACHVGGGTATCTAATCC) were used for 1st stage PCR to amplify the 16S rRNA gene. To add dual indices and Illumina sequencing adapters to the 1st stage amplicons, 2nd stage PCR was performed using the Nextera XT Index Kit (Illumina). The prepared libraries were then pooled and sequenced using the MiSeq sequencer with 2 × 250-bp paired-end option (Illumina). The sequence data have been deposited in the NCBI Short Read Archive under the accession number SRX3195509. The resultant sequencing reads were analyzed using the QIIME pipeline [25] and Greengenes 16S database 13_8 [26]. USEARCH 7 [27] was used for quality filtering of singletons and ref-based chimera checking. As a result, 13,000–61,000 reads were obtained from the individual samples. To equalize the sequencing depth among samples, random subsampling of 10,000 reads for each sample was conducted. All the data presented in this study were calculated from this subset data. The beta-diversity of the microbiome was calculated using Fast UniFrac interface [28] and visualized using principal coordinate analysis (PCoA). The Unifrac distance-based inter- and intra-dissimilarity depending on experimental groups was determined using the ANOSIM test. The differences in taxa abundance, depending on categorical metadata, were evaluated using Hotelling's *t*-test (p-value ≤ 0.05) and LEfSe analyses (LDA score ≥ 2.50) [29]. The taxa identified at the species level based on the Greengene database were further evaluated using the EzTaxon-e database [30].

Mouse Gene Expression Analyses

RNA was extracted from the liver tissue using an RNeasy Lipid Tissue Mini Kit (Qiagen, Germany). RNA labeling and hybridization were performed using the Agilent One-Color Microarray-Based Gene Expression Analysis protocol (ver. 6.5; Agilent Technologies, USA). The prepared hybridization solution was then dispensed into a gasket slide and assembled for the Agilent SurePrint G3 Mouse GE 8X60K, V2 Microarrays (Agilent); the slides were then incubated for 17 h at 65°C. The hybridized array was immediately scanned using an Agilent Microarray Scanner D (Agilent) and analyzed using Agilent Feature Extraction Software ver. 11.0.1.1. The selected expression value was logarithmically transformed and normalized using the quantile method. Statistical significance of the expression data was determined using fold change. Gene-enrichment and functional annotation analysis were performed using gene ontology [31] and KEGG pathway analysis [32].

Microbiome-Gene Interaction Analyses

Correlation coefficients between intestinal bacteria and host genes were determined. For this, differentially expressed genes with >2-fold change and bacterial taxa showing differential abundance depending on metadata with a p-value < 0.05 were selected. Pearson correlation coefficients were calculated between pairs of expression level and bacterial abundance (%). Permutation was performed 1,000 times, and the p value was corrected using the Benjamin method using the R program [33], and gene-bacterial pairs with p-values < 0.05 were selected. The microbe-host interaction in the SHAM-HF and OVX groups were selected and found to be enriched in the KEGG pathway. The correlation was visualized using Cytoscape [34].

Results

Phenotypic Difference between Ovariectomy-Induced and Diet-Induced Obesity

The obesity-related indices measured in this study revealed phenotypic similarities between the ovariectomized and high-fat diet groups. The final body weight and amount of adipose tissue in mice in the OVX, SHAM-HF, and OVX-HF groups were significantly increased relative to the SHAM group (Table 1). The highest weight gain was observed in the OVX-HF group, followed by the SHAM-HF and OVX

Table 1. Obesity-related indices showing effects of ovariectomy and/or high-fat (HF) diet on the mouse phenotype.

	Final body weight (g)	Total white fat mass (g/100 g body weight)	Triglyceride (mg/dl)	Total cholesterol (mg/dl)	HDL-cholesterol (mg/dl)	LDL-cholesterol[a] (mg/dl)	AI [b]	CRF [c]
SHAM	29.96 ± 2.13$^{\#}$	0.962 ± 0.473$^{\#}$	45.3 ± 13.6	65.5 ± 23.3	45.7 ± 5.0	30.9 ± 5.1	0.434	1.434
OVX	41.44 ± 1.52*	6.559 ± 0.967*	52.6 ± 7.7	82.2 ± 13.7	49.7 ± 5.7	45.1 ± 9.1	0.655	1.655
SHAM-HF	53.13 ± 3.88$^{*,\#}$	10.33 ± 2.07*	56.6 ± 5.3	105.7 ± 25.3	39.8 ± 2.6	78.0 ± 4.4$^{*,\#}$	1.658$^{*,\#}$	2.658$^{*,\#}$
OVX-HF	57.54 ± 3.84$^{*,\#}$	11.94 ± 1.69$^{*,\#}$	68.7 ± 10.4	128.6 ± 26.6	44.7 ± 3.6	95.7 ± 12.3$^{*,\#}$	1.880$^{*,\#}$	2.880$^{*,\#}$

Data are presented as the mean ± standard error; *p < 0.05 vs. SHAM group; $^{\#}p$ < 0.05 vs. OVX group.

[a]LDL-cholesterol = [total cholesterol - (HDL-cholesterol – triglyceride / 5)].

[b]AI (atherogenic index) = (total cholesterol - HDL-cholesterol) / HDL-cholesterol.

[c]CRF (cardiac risk factor) = total cholesterol / HDL-cholesterol.

groups. The OVX, OVX-HF, and SHAM-HF groups tended to have increased triglyceride, total cholesterol, and LDL-cholesterol levels, AI, and CRF and decreased HDL-cholesterol levels compared with the control group (SHAM), but these differences were not statistically significant in some cases. The LDL-cholesterol levels, AI, and CRF were significantly increased in the high-fat diet-treated groups (SHAM-HF and OVX-HF).

Decreased Gut Microbiome Diversity by Ovariectomy

Bacterial counts and diversity in the experimental groups were lower than those in the control group (SHAM) (Fig. S1). In both the SHAM-HF and OVX groups, the number of observed OTUs and Shannon diversity were decreased. However, in the OVX-HF group, those numbers recovered to levels close to those of the control group.

Ovariectomy and High-Fat Diet Resulted in Similar Microbiome Structures

The experimental treatments had a large impact on the bacterial community structure. The similarities in the microbiome among samples were estimated based on weighted UniFrac distance, and the results of PCoA showed that the overall bacterial communities of the experimental groups were clearly differentiated from the control group (ANOSIM statistic R = 0.4509, p-value = 0.001) (Fig. 1). Remarkably, the differences in the microbiome caused by ovariectomy (red spots) were very similar to those caused by the high-fat diet (blue spots) (ANOSIM $p > 0.05$). The distribution areas of the two experimental groups were superimposed in the middle part. The overall bacterial community in the OVX-HF group (purple spots) showed a similar profile with the other two experimental groups (ANOSIM $p > 0.3$), but showed a larger variation width than the SHAM-HF and OVX groups (Wilcox t-test $p = 0.005$).

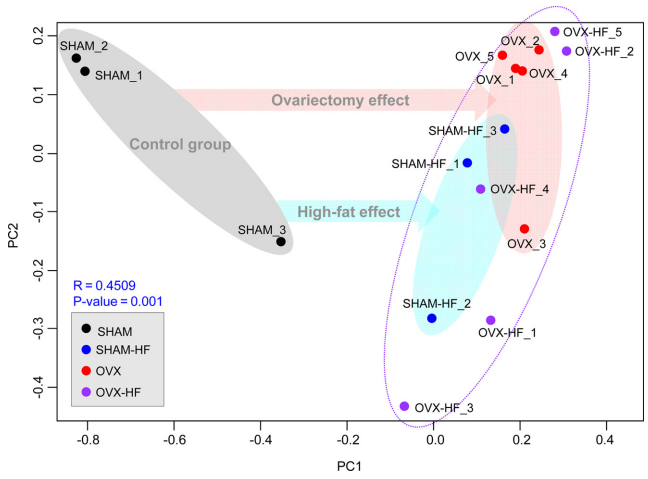

Fig. 1. Differences in the microbiome between samples quantified using the weighted UniFrac distance and principal coordinate analysis.

Bifidobacterium Species Were Exclusively Detected in the Ovariectomized Mice

Seven bacterial phyla were detected in the mice in the control and experimental groups (Fig. 2). In the control group, the dominant bacterial group was the phylum Bacteroidetes. In the OVX and SHAM-HF groups, the phylum Firmicutes was dominant and the phylum Actinobacteria showed increased abundance. At the phylum level, changes in the microbiome induced by ovariectomy were not different from those induced by the high-fat diet. However, the OVX-HF group showed differences compared with the other groups with increased abundance of Verrucomicrobia and Proteobacteria species.

Forty-one genus-level taxa were detected from the gut samples of the mice (Table S1). In the control group, Bacteroidales S24-7 and *Bacteroides* species were abundant. In the SHAM-HF group, *Lactobacillus* and Clostridiales OTUs were dominant. In the OVX group, *Lactobacillus* was dominant and the abundance of *Akkermansia* species was increased in the OVX-HF group.

Bacterial taxa showing differences between groups were identified by LEfse analyses and statistical evaluation (Fig. 3). The gut microbiome of the mice in the SHAM group was characterized by the exclusive presence of four bacteria: *Prevotella* species (LDA = 4.07, p-value = 0.036), *Bacteroides acidifaciens* (LDA = 4.05, p-value = 0.036), *Bacteroidales* S24-7 (LDA = 4.69, p-value = 0.036), and *Rikenellaceae* species

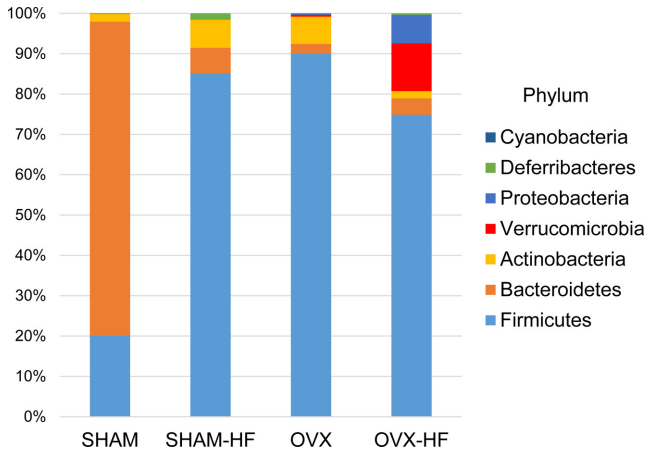

Fig. 2. Composition of the gut microbiome of mice at the bacterial phylum level.

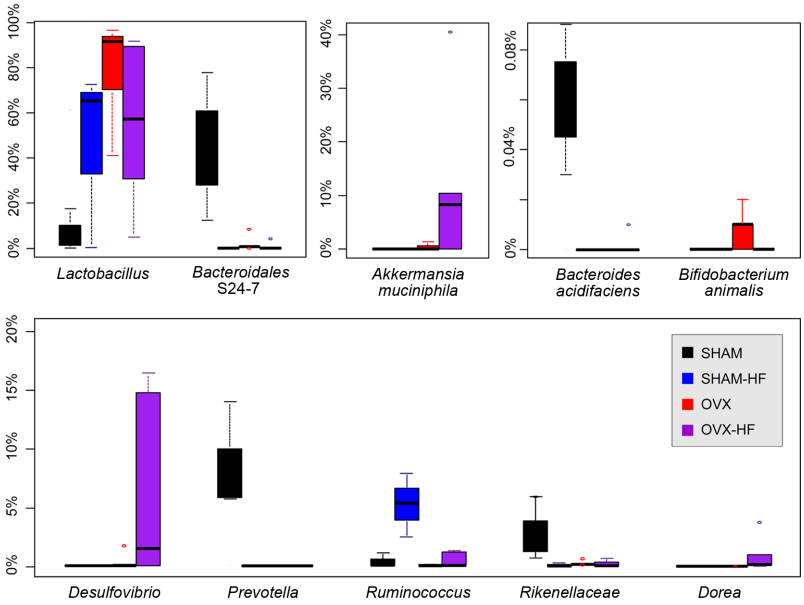

Fig. 3. Relative abundance of different bacterial taxa showing differences between different experimental groups.
The solid black lines represent the medians, and the circles are outliers. Bars denote the minimum and maximum values excluding the outliers.

(LDA = 3.70, *p*-value = 0.025). The abundance of these bacteria was decreased in the experimental groups in this study. The proportion of *Lactobacillus* species was significantly increased in all the treatment groups compared with that in the SHAM control group. The SHAM-HF group was characterized by an increase in *Lactobacillus* (LDA = 4.84, *p*-value = 0.043) and *Ruminococcus* (LDA = 4.08, *p*-value = 0.039) abundance. The OVX group showed increased abundance of *Lactobacillus* species (LDA = 4.68, *p*-value = 0.049) and the exclusive presence of *Bifidobacterium animalis* (LDA = 3.36, *p*-value = 0.043). The OVX-HF group was characterized by increased abundance of *Lactobacillus* (LDA = 4.68, *p*-value = 0.05), *Dorea* (LDA = 3.56, *p*-value = 0.024), *Akkermansia muciniphila* (LDA = 4.37, *p*-value = 0.043), and *Desulfovibrio* species (LDA = 4.12, *p*-value = 0.05).

Ovariectomy Induced Differential Gene Expression

Gene expression in the liver tissue was significantly different in the OVX group compared with the SHAM control group (Fig. 4). The result of the enrichment map test using KEGG pathways showed that 177 metabolic pathways differed in the OVX group compared with that in the SHAM control group. In particular, the gene expression of estrogen signaling pathways differed significantly in the OVX group compared with the SHAM control group. However, the estrogen signaling pathways were not different in the OVX-HF group compared with the SHAM-HF group.

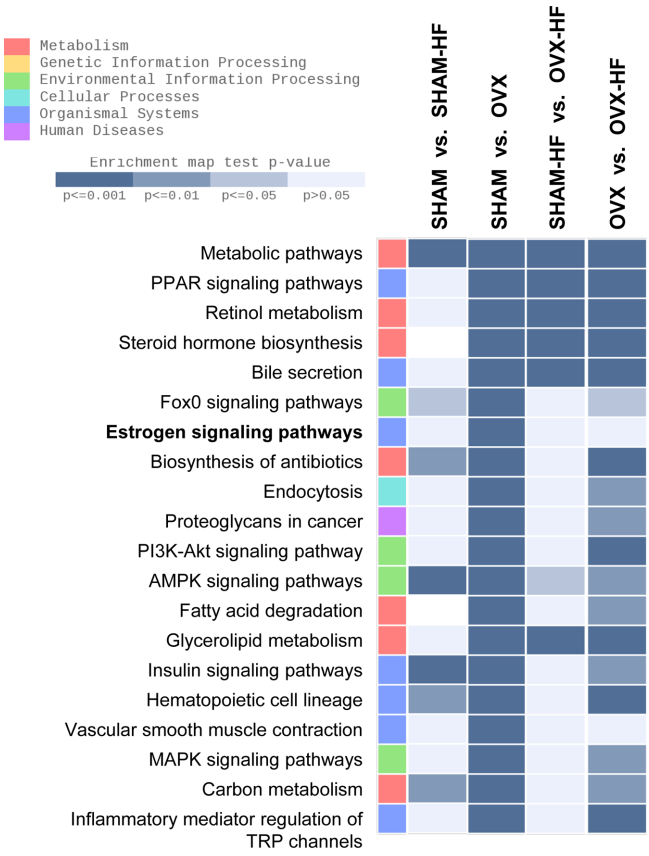

Fig. 4. Top 20 KEGG pathways enriched in the four groups.
The statistical significance was calculated using the modified Fisher's exact test.

Microbiome-Host Interaction in the Ovariectomized Mice

The microbiome-host interaction in the ovariectomized mice was compared with that of mice on high-fat diet-fed (Fig. 5). With regard to the high-fat diet-related gene expression, *Ruminococcus*, *Dorea* species, and *A. muciniphila* showed broad correlations with genes of the metabolic pathway, MAPK signaling pathway, AMPK signaling pathway, and FoxO signaling pathway. With regard to ovariectomy-related gene expression, *Lactobacillus* species showed broad interaction with host metabolism, including metabolic pathways, antibiotic biosynthesis pathways, FoxO signaling pathway, glycerophospholipid metabolism pathway, and steroid hormone biosynthesis pathway. *Akkermansia muciniphila* was related to *Pik3ca* and *Lgf1*, which belong to the estrogen signaling pathway and ovarian steroidogenesis pathway, and to *Cyp26b1*, *Nnmt*, *Pnpla3*, and *Ptgds*, all of which are involved in metabolic pathways.

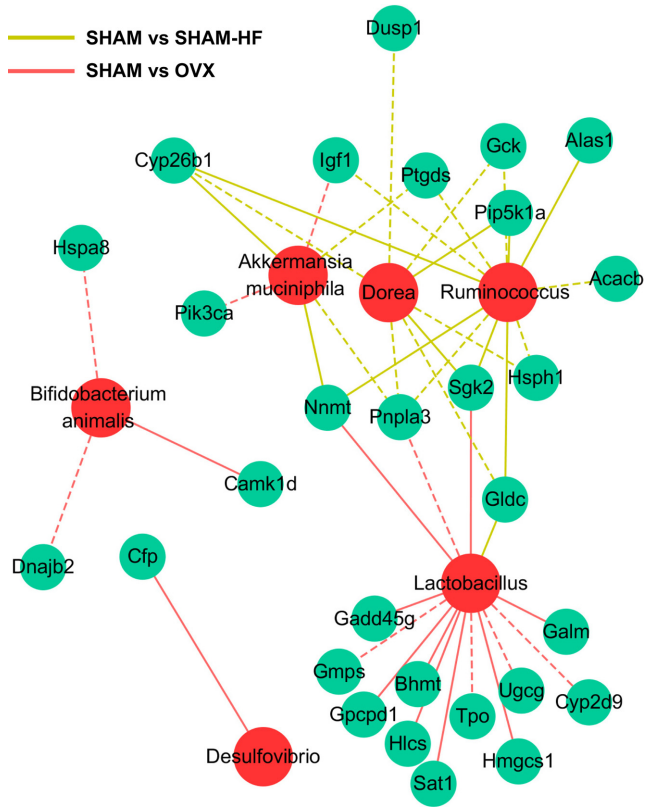

Fig. 5. Bacteria-gene expression network of ovariectomized mice compared with that of high-fat diet-fed mice.

Red circles correspond to bacteria; green circles correspond to differentially expressed genes of KEGG maps; yellow lines indicate bacteria-gene correlation in the high-fat diet-fed mice; red lines indicate bacteria-gene correlation in the ovariectomized mice; solid lines indicate positive correlation; dashed lines indicate negative

In contrast, *Bifidobacterium animalis* and *Desulfovibrio* species showed narrow interaction with host female hormone metabolism. *B. animalis* was related to *Hspa8*, *Dnajb2*, and *Camk1d*, which belong to the estrogen signaling pathway, sterol biosynthetic pathway, and oxytocin signaling pathway. *Desulfovibrio* species showed single pairwise relationship with *Cfp*, the gene coding a component of the innate immune system.

Discussion

A 15–23% increase in body weight observed in ovariectomized animals has been reported previously [35, 36], and the same level of weight gain was also confirmed in the ovariectomized mice in this study. The overall change in the microbiome profile depending on ovariectomy was also consistent with these previous reports. The decrease in the abundance of phylum Bacteroidetes (from 78% to 2%) and increase in the abundance of phylum Firmicutes (from 20% to 90%) observed in this study were also consistent with the changes observed in previous studies. At a lower taxonomic level, we observed a decrease in the abundance of Ruminococcaceae, Rikenellaceae, Clostridia, Bacteroidales S24-7, *Bacteroides*, and *Prevotella* species and an increase in the abundance of *Lactobacillus* species, which was also in line with a previous report [35]. However, the details of the microbiome changes observed in our study were different from those observed in previous studies. Several bacterial taxa such as *Moryella*, *Sporobacter*, *Barnesiella*, *Eggerthella*, Porphyromonadaceae, and *Oscillospira*, which have been reported to show differential abundance upon ovariectomy [35], were not detected or showed no significant differences (between OVX and SHAM groups) in our study.

Additionally, we found that the high-fat diet increased the proportion of phylum Firmicutes (from 20% to 85%) and decreased the proportion of phylum Bacteroidetes (from 78% to 6%), which were consistent with the reports of previous animal and human studies [37–39]. At a lower taxonomic level, a decrease in the abundance of Ruminococcaceae, Rikenellaceae, Lachnospiraceae, *Bacteroides*, and *Prevotella* species and an increase in the abundance of *Lactobacillus* species were observed in the SHAM-HF group in our study; this result was also in line with previous reports [40, 41]. The OVX-HF group showed a similar microbiome composition as the OVX group except for the presence of a few different taxa.

We expected the differential expression of estrogen signaling pathways in OVX treatment. This was observed as expected in the comparison of the OVX with the SHAM

groups. However, the differential expression was not observed in the comparison of OVX-HF with SHAM-HF. The number of differential metabolic processes between SHAM_HF and OVX_HF was also low, at 17 pathways compared with the 177 pathways in the OVX versus the SHAM groups. This phenomenon was in line with the microbiome data. The overall bacterial profiles showed a significant difference in the comparison of OVX with SHAM, but the bacterial profiles of SHAM_HF and OVX_HF were similar.

Bifidobacterium animalis, an ovariectomy-specific bacterium, showed strong correlations with three genes—*Hspa8* (heat shock cognate Hsc73 protein), *Dnajb2* (DnaJ homolog superfamily B member 2), and *Camk1d* (calcium/calmodulin-dependent protein kinase ID). The expression of Hspa8, which is known to be related with ovarian hormones [42], was found to be elevated in the OVX mice and showed positive correlation with an increase in the abundance of *B. animalis*. Dnajb2, a protein involved in the sterol biosynthetic process, also showed increased expression accordingly. In contrast, the expression of Camk1d, a protein involved in the onset of breast cancer and the oxytocin signaling pathway, was decreased in the OVX group, showing a negative correlation with the abundance of *B. animalis*. The gene-bacterial correlation observed here suggests a possible role of *B. animalis* in female hormone regulation; however, further studies are required to confirm this possibility.

Furthermore, *Desulfovibrio*, *Dorea*, and *A. muciniphila* species showed a correlation with both high-fat diet and ovariectomy (OVX-HF group). *Desulfovibrio* abundance was found to be positively correlated with Cfp (complement factor properdin), a component of the innate immune system that has been reported to show upregulation upon ovariectomy [43]. Furthermore, *A. muciniphila* abundance showed a negative correlation with two genes, *Pik3ca* (phosphatidylinositol 3-kinase catalytic alpha polypeptide) and *Lfg1* (insulin-like growth factor 1), but more correlation was observed with metabolic pathway genes (*Cyp26b1*, *Nnmt*, *Pnpla3*, and *Ptgds*) whose expression is related to a high-fat diet than with genes related to ovariectomy. With regard to *Dorea* species, although their proportion increased in the OVX-HD group, the gene-bacterial correlation was for genes of the metabolic pathways. Considering the data available about the relief function of *A. muciniphila* in metabolic dysfunctions [44, 45], the increase in the abundance of *A. muciniphila* and *Dorea* species in this group is likely due to the high-fat diet than due to the ovariectomy.

Comprehensively speaking, the overall microbiome trend was similar in both dietary-induced obesity and postmenopausal obesity, but *B. animalis* was found to exist exclusively in postmenopausal obesity. Several other bacteria, including *Dorea*, *A. muciniphila*, and *Desulfovibrio* species, showed an additional increase in their abundance observed in the OVX-HF group relative to that in the OVX group; that is, a high-fat diet further enhanced the ovariectomy-induced increase in the abundance of these species. However, with regard to bacteria-gene interactions, only *B. animalis* appeared to be specifically correlated with female estrogen metabolism. The results of this study indicate that menopausal obesity is characterized by marker species that differ from those of diet-induced obesity, and that these marker species show correlation with female hormone metabolism genes.

Conflict of Interest

The authors have no financial conflicts of interest to declare.

Acknowledgments

This study was carried out with the support of the Cooperative Research Program for Agricultural Science & Technology Development (Project No. PJ010975), Rural Development Administration, Republic of Korea.

References

1. McKinlay SM, Brambilla DJ, Posner JG. 1992. The normal menopause transition. *Maturitas* **14:** 103-115.
2. Eriksen EF, Colvard DS, Berg NJ, Graham ML, Mann KG, Spelsberg TC, *et al.* 1988. Evidence of estrogen receptors in normal human osteoblast-like cells. *Science* **241:** 84-86.
3. Lindsay R, Hart DM, Aitken JM, MacDonald EB, Anderson JB, Clarke AC. 1976. Long-term prevention of postmenopausal osteoporosis by oestrogen. Evidence for an increased bone mass after delayed onset of oestrogen treatment. *Lancet* **1:** 1038-1041.
4. Riggs BL, Khosla S, Melton LJ 3rd. 1998. A unitary model for involutional osteoporosis: estrogen deficiency causes both type I and type II osteoporosis in postmenopausal women and contributes to bone loss in aging men. *J. Bone Miner. Res.* **13:** 763-773.
5. Paganini-Hill A, Henderson VW. 1994. Estrogen deficiency and risk of Alzheimer's disease in women. *Am. J. Epidemiol.* **140:** 256-261.
6. Yue X, Lu M, Lancaster T, Cao P, Honda S, Staufenbiel M, *et al.* 2005. Brain estrogen deficiency accelerates Aβ plaque

formation in an Alzheimer's disease animal model. *Proc. Natl. Acad. Sci. USA* **102:** 19198-19203.
7. Ainslie DA, Morris MJ, Wittert G, Turnbull H, Proietto J, Thorburn AW. 2001. Estrogen deficiency causes central leptin insensitivity and increased hypothalamic neuropeptide Y. *Int. J. Obes. Relat. Metab. Disord.* **25:** 1680-1688.
8. Lovejoy JC, Champagne CM, de Jonge L, Xie H, Smith SR. 2008. Increased visceral fat and decreased energy expenditure during the menopausal transition. *Int. J. Obes.* **32:** 949-958.
9. Shimizu H, Shimomura Y, Nakanishi Y, Futawatari T, Ohtani K, Sato N, *et al*. 1997. Estrogen increases in vivo leptin production in rats and human subjects. *J. Endocrinol.* **154:** 285-292.
10. Carr MC. 2003. The emergence of the metabolic syndrome with menopause. *J. Clin. Endocrinol. Metab.* **88:** 2404-2411.
11. Dosi R, Bhatt N, Shah P, Patell R. 2014. Cardiovascular disease and menopause. *J. Clin. Diagn. Res.* **8:** 62-64.
12. Hu FB, Grodstein F, Hennekens CH, Colditz GA, Johnson M, Manson JE, *et al.* 1999. Age at natural menopause and risk of cardiovascular disease. *Arch. Intern. Med.* **159:** 1061-1066.
13. Ramezani Tehrani F, Behboudi-Gandevani S, Ghanbarian A, Azizi F. 2014. Effect of menopause on cardiovascular disease and its risk factors: a 9-year follow-up study. *Climacteric* **17:** 164-172.
14. Coylewright M, Reckelhoff JF, Ouyang P. 2008. Menopause and hypertension: an age-old debate. *Hypertension* **51:** 952-959.
15. Rappelli A. 2002. Hypertension and obesity after the menopause. *J. Hypertens. Suppl.* **20:** S26-S28.
16. Nelson HD, Humphrey LL, Nygren P, Teutsch SM, Allan JD. 2002. Postmenopausal hormone replacement therapy: scientific review. *JAMA* **288:** 872-881.
17. Hummelen R, Macklaim JM, Bisanz JE, Hammond JA, McMillan A, Vongsa R, *et al.* 2011. Vaginal microbiome and epithelial gene array in post-menopausal women with moderate to severe dryness. *PLoS One* **6:** e26602.
18. Brotman RM, Shardell MD, Gajer P, Fadrosh D, Chang K, Silver MI, *et al.* 2014. Association between the vaginal microbiota, menopause status, and signs of vulvovaginal atrophy. *Menopause* **21:** 450-458.
19. Cauci S, Driussi S, De Santo D, Penacchioni P, Iannicelli T, Lanzafame P, *et al.* 2002. Prevalence of bacterial vaginosis and vaginal flora changes in peri- and postmenopausal women. *J. Clin. Microbiol.* **40:** 2147-2152.
20. Fuhrman BJ, Feigelson HS, Flores R, Gail MH, Xu X, Ravel J, *et al*. 2014. Associations of the fecal microbiome with urinary estrogens and estrogen metabolites in postmenopausal women. *J. Clin. Endocrinol. Metab.* **99:** 4632-4640.
21. Flores R, Shi J, Fuhrman B, Xu X, Veenstra TD, Gail MH, *et al.* 2012. Fecal microbial determinants of fecal and systemic estrogens and estrogen metabolites: a cross-sectional study. *J. Transl. Med.* **10:** 253.
22. Menon R, Watson SE, Thomas LN, Allred CD, Dabney A, Azcarate-Peril MA, *et al*. 2013. Diet complexity and estrogen receptor beta status affect the composition of the murine intestinal microbiota. *Appl. Environ. Microbiol.* **79:** 5763-5773.
23. Kwa M, Plottel CS, Blaser MJ, Adams S. 2016. The intestinal microbiome and estrogen receptor-positive female breast cancer. *J. Natl. Cancer Inst.* **108:** djw029.
24. Brahe LK, Le Chatelier E, Prifti E, Pons N, Kennedy S, Hansen T, *et al.* 2015. Specific gut microbiota features and metabolic markers in postmenopausal women with obesity. *Nutr. Diabetes* **5:** e159.
25. Lawley B, Tannock GW. 2017. Analysis of 16S rRNA gene amplicon sequences using the QIIME software package. *Methods Mol. Biol.* **1537:** 153-163.
26. DeSantis TZ, Hugenholtz P, Larsen N, Rojas M, Brodie EL, Keller K, *et al.* 2006. Greengenes, a chimera-checked 16S rRNA gene database and workbench compatible with ARB. *Appl. Environ. Microbiol.* **72:** 5069-5072.
27. Edgar RC. 2010. Search and clustering orders of magnitude faster than BLAST. *Bioinformatics* **26:** 2460-2461.
28. Hamady M, Lozupone C, Knight R. 2010. Fast UniFrac: facilitating high-throughput phylogenetic analyses of microbial communities including analysis of pyrosequencing and PhyloChip data. *ISME J.* **4:** 17-27.
29. Segata N, Izard J, Waldron L, Gevers D, Miropolsky L, Garrett WS, *et al*. 2011. Metagenomic biomarker discovery and explanation. *Genome Biol.* **12:** R60.
30. Yoon SH, Ha SM, Kwon S, Lim J, Kim Y, Seo H, *et al*. 2017. Introducing EzBioCloud: a taxonomically united database of 16S rRNA gene sequences and whole-genome assemblies. *Int. J. Syst. Evol. Microbiol.* **67:** 1613-1617.
31. Ashburner M, Ball CA, Blake JA, Botstein D, Butler H, Cherry JM, *et al.* 2000. Gene ontology: tool for the unification of biology. The Gene Ontology Consortium. *Nat. Genet.* **25:** 25-29.
32. Kanehisa M, Furumichi M, Tanabe M, Sato Y, Morishima K. 2017. KEGG: new perspectives on genomes, pathways, diseases and drugs. *Nucleic Acids Res.* **45:** D353-D361.
33. The R project for statistical computing. Available from http://www.r-project.org. Accessed 18 September 2017.
34. Cline MS, Smoot M, Cerami E, Kuchinsky A, Landys N, Workman C, *et al.* 2007. Integration of biological networks and gene expression data using Cytoscape. *Nat. Protoc.* **2:** 2366-2382.
35. Cox-York KA, Sheflin AM, Foster MT, Gentile CL, Kahl A, Koch LG, *et al.* 2015. Ovariectomy results in differential shifts in gut microbiota in low versus high aerobic capacity rats. *Physiol. Rep.* **3**: e12488.
36. Keenan MJ, Janes M, Robert J, Martin RJ, Raggio AM, McCutcheon KL, *et al.* 2013. Resistant starch from high amylose maize (HAM-RS2) reduces body fat and increases gut bacteria in ovariectomized (OVX) rats. *Obesity* **21:** 981-984.
37. Hildebrandt MA, Hoffmann C, Sherrill-Mix SA, Keilbaugh SA, Hamady M, Chen YY, *et al.* 2009. High-fat diet determines the composition of the murine gut microbiome independently

of obesity. *Gastroenterology* **137:** 1716-1724.e1-2.
38. Turnbaugh PJ, Baeckhed F, Fulton L, Gordon JI. 2008. Diet-induced obesity is linked to marked but reversible alterations in the mouse distal gut microbiome. *Cell Host Microbe* **3:** 213-223.
39. Wu GD, Chen J, Hoffmann C, Bittinger K, Chen YY, Keilbaugh SA, *et al.* 2011. Linking long-term dietary patterns with gut microbial enterotypes. *Science* **334:** 105-108.
40. Rabot S, Membrez M, Blancher F, Berger B, Moine D, Krause L, *et al.* 2016. High fat diet drives obesity regardless the composition of gut microbiota in mice. *Sci. Rep.* **6:** 32484.
41. Liu TW, Park YM, Holscher HD, Padilla J, Scroggins RJ, Welly R, *et al.* 2015. Physical activity differentially affects the cecal microbiota of ovariectomized female rats selectively bred for high and low aerobic capacity. *PLoS One* **10:** e0136150.
42. Krebs CJ, Jarvis ED, Pfaff DW. 1999. The 70-kDa heat shock cognate protein (Hsc73) gene is enhanced by ovarian hormones in the ventromedial hypothalamus. *Proc. Natl. Acad. Sci. USA* **96:** 1686-1691.
43. Sarvari M, Kallo I, Hrabovszky E, Solymosi N, Liposits Z. 2014. Ovariectomy and subsequent treatment with estrogen receptor agonists tune the innate immune system of the hippocampus in middle-aged female rats. *PLoS One* **9:** e88540.
44. Everard A, Belzer C, Geurts L, Ouwerkerk JP, Druart C, Bindels LB, *et al.* 2013. Cross-talk between *Akkermansia muciniphila* and intestinal epithelium controls diet-induced obesity. *Proc. Natl. Acad. Sci. USA* **110:** 9066-9071.
45. Shin NR, Lee JC, Lee HY, Kim MS, Whon TW, Lee MS, *et al.* 2014. An increase in the *Akkermansia* spp. population induced by metformin treatment improves glucose homeostasis in diet-induced obese mice. *Gut* **63:** 727-735.